13th IEA Heat Pump Conference
April 26-29, 2021 Jeju, Korea

Part Load Capability of a High Temperature Heat Pump with Reversed Brayton Cycle

Johannes Oehler[a1], Jens Gollasch[a], A. Phong Tran[a], Eberhard Nicke[a]

[a] Institute of Low-Carbon Industrial Processes, German Aerospace Center, 03044 Cottbus, Germany

Deutsches Zentrum für Luft- und Raumfahrt
German Aerospace Center

Abstract

This paper studies the part load behavior and capability of a high temperature heat pump that operates with the Brayton cycle. A novel concept of a high temperature heat pump which is currently under construction in Cottbus (Germany) is presented. It goes far beyond temperature levels of current high temperature heat pumps and will provide process heat at above 250 °C. The heat pump uses a closed Brayton cycle driven by axial turbomachinery and provides up to 200 kW of thermal energy. The thermal output can be adjusted by variation of compressor shaft speed, use of internal recuperation and additionally by variation of the fluid inventory. The latter allows operation of our prototype within a broad part load range down to 25 % of the nominal power at nearly constant efficiencies and output temperatures. Brayton cycle heat pumps can be adapted to a wide range of industrial processes and enable highly efficient thermal energy storage systems to balance grid fluctuations.

Keywords: high temperature heat pump; reverse Brayton cycle; fluid inventory control; process heat; electrification

1. Introduction

Industrial processes account for about 25 % of the primary energy used and 20 % of greenhouse gas emissions in the EU-28 countries. Two thirds of this energy are used to meet the process heat demand [1]. Together with space heating in domestic and industrial applications heating and cooling account for 51 % of the final energy consumption in Europe [2]. Current technology relies mainly on fossil fuels such as coal, natural gas and petroleum products [3]. In order to transition to a climate-neutral economy by 2050 which is the declared goal of the European Union [4] all these heat requirements must be met by net zero carbon technologies within 30 years. Heat pumps have been identified as a key technology towards this goal [5].

When using electricity from conventional fossil sources, power to heat technologies are only interesting if either highly efficient or in applications where combustion and emissions are undesired. Otherwise, the losses and the complexity of two conversions from fuel to electricity to heat can hardly be justified. Therefore, conventional heat pumps for low temperature applications such as domestic warm water and space heating are the only field where heat pumps find widespread use as of now [6].

Heat pumps are an important component in energy storage concepts and a possible power-on-demand tool in a more flexible energy system [5, 7, 8]. Efficient part load operation increases the grid balancing capability of heat pumps and is also a selling point for heat pumps in industrial processes where they compete with boilers. Variation of the working pressure is a common tool for changing the power level of a thermodynamic cycle process without having to adapt the geometry [9, 10]. In this paper, the part load capability of a closed loop Brayton cycle heat pump using fluid inventory control is analyzed.

[1] Corresponding author. Tel.: +49 30 67055 8155; *E-mail address:* johannes.oehler@dlr.de

Nomenclature

Abbreviations

DLR	German Aerospace Center
FI	Fluid inventory
FIC	Fluid inventory control
GTlab	Gas Turbine Laboratory
HT	High temperature
HTHE	High temperature heat exchanger
HTHP	High temperature heat pump
LT	Low temperature
LTHE	Low temperature heat exchanger
NTU	Number of transfer units
PTC	Performance Test Code
SSC	Shaft speed control

Variables

a	Fraction of Reynolds independent losses [-]
A	Flow area [m²]
c	Flow velocity [m/s]
COP	Coefficient of performance [-]
M_{Fluid}	Fluid mass [kg]
$\dot{m}$	Mass flow [kg/s]
n	Reynolds dependency of losses [-]
P_C	Compressor power [W]
P_T	Turbine power [W]
p	Total pressure [Pa]
$\dot{Q}$	Heat flow [W]
q_c	Specific heat absorbed at heat source [J/kg]
q_h	Specific heat provided at heat sink [J/kg]
Re	Reynolds number [-]
T_0	Heat source temperature [K]
T_1	Compressor inlet temperature [K]
T_2	Compressor outlet temperature [K]
T_3	Turbine inlet temperature [K]
T_4	Turbine outlet temperature [K]
w	Specific work [J/kg]
V	Volume [m³]
Δp	Pressure drop [Pa]
ζ	Loss coefficient [-]
η	Efficiency [-]
η_{th}	Thermal efficiency [-]
κ	Isentropic exponent [-]
ρ	Density [kg/m³]

Table 1 shows different technologies to electrify process heat demand. They all rely on renewable electricity which must be generated emission-free in order to reach a climate-neutral economy.

Using resistance heating one unit of electrical power is converted to the same amount of thermal energy. When burning substitute natural gas (SNG) or green hydrogen, conversion losses cannot be avoided [11]. Less than one kWh of process heat is generated per kWh of renewable electricity used. With heat pump technology, it is possible to convert one unit of renewable electricity into several units of usable thermal energy. In order to decarbonize process heat demand efficiently, heat requirements at low temperature levels should be met with emission-free technologies first. Process heat at high temperature levels needs a larger investment of renewable electricity per energy unit of heat which can be seen from the low conversion ratio in high temperature applications (see Table 1). Rehfeldt et al. [3] show that a relevant portion of process heat is required at temperature levels from 100 °C to 500 °C.

Heat pumps for sink temperatures of up to 160 °C are already available on the market [6]. The feasibility of heat pumps with sink temperatures as high as 280 °C [12] and 465 °C [7] has been proven utilizing currently available compressor technology. Zühlsdorf et al. [12] suggest a reverse Brayton or Rankine cycle for heat-pumps with very high sink temperatures (> 250 °C) and suggest that coefficients of performance (COP) of nearly two are possible. The German Aerospace Center's (DLR) Institute of Low-Carbon Industrial Processes is currently constructing prototype heat pumps with sink temperatures above 250 °C researching both Rankine and Brayton cycle technology. This paper focuses on the reverse Brayton cycle.

Table 1: Overview of power to heat technologies for process heat demand

Technology	Temperature level	Conversion ratio from net electrical power (COP for heat pumps)	Heating demand for industrial processes in Europe [3]**
Green hydrogen	only material limit	70% [11]	3726 PJ (> 500 °C)
Green gas (SNG)	only material limit	55% [11]	
Resistance heating	At least 850 °C [13]	<100 %	
Ultra-high temperature heat pump	250-500 °C	130-200 %* [7] [12]	2542 PJ (100 – 500 °C)
High temperature heat pump	100-160 °C	200-500 %* [6]	
Conventional heat pump	20-100 °C	300-600%* [6]	821 PJ (<100°C)

* Conversion ratio strongly depends on heat source temperature

** numbers for EU-28 plus Norway, Switzerland and Iceland in 2012, heat demand for space heating not included

2. Thermodynamics of high temperature heat pumps

The reversed Brayton and Rankine cycles are the thermodynamic models of the most commonly used closed cycle compression heat pumps. The Rankine process is preferred in refrigeration and heat pump processes in the temperature range from -40 °C to 160 °C [6, 14]. It makes use of the phase transition of its working fluid (refrigerant) but is for this reason limited by the physical properties of the refrigerant. The Brayton-process has no phase transition and no temperature limit if air or noble gas is used as a working fluid.

2.1. Brayton process

The Brayton process models a gas turbine process. Operating it reversely (counterclockwise) turns it into a heat pump [14]. Isentropic compression ($T_1 \rightarrow T_2$) happens at a higher temperature level than isentropic expansion ($T_3 \rightarrow T_4$). Sensible heat q_h is provided during an isobaric state change between temperatures T_2 and T_3. The cycle absorbs sensible heat q_c from the environment in an isobaric state change from T_4 to T_1. T_1 is therefore limited to the temperature of the heat source T_0.

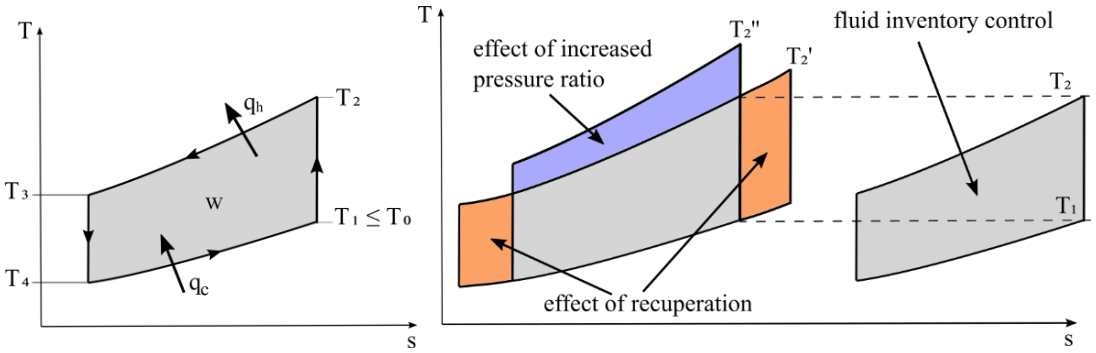

Figure 1: Temperature-entropy diagram of the Brayton cycle (left) and effect through variation of pressure ratio, recuperation or fluid inventory control adapted from [9, 14] (right)

The power turnover of a Brayton cycle can be changed in two ways. By changing the similarity parameters of the cycle and thereby the specific work w or by varying the amount of working fluid exercising the thermodynamic process. Changing the pressure ratio or introducing recuperation affects the temperature levels and the area inside the loop process which represents the specific work w (see Figure 1). With means of fluid inventory control, the process can be shifted sideward in the T-s diagram. When shifted to the right to lower pressure isobars the specific work and temperatures remain constant but the amount of working fluid is reduced. The total power as product of specific work and mass flow is also decreased. Fluid inventory control therefore enables part load operation at constant process temperatures.

2.2. Coefficient of performance

The coefficient of performance (COP) of heat pumps is defined as the ratio between heat delivered from the cycle to the heat sink q_h and work consumed in the thermodynamic cycle process w. The COP is the inverse of the thermal efficiency η_{th} of the equivalent thermal engine [14].

$$COP = \frac{q_h}{w} = \frac{1}{\eta_{th}} \tag{1}$$

For the ideal Brayton cycle with constant isentropic exponent κ the specific work w can be expressed as the difference between heat provided q_h and heat absorbed q_c and $\mathrm{COP}_{\mathrm{Brayton}}$ is a sole function of the compressor inlet temperature T_1 and the compressor outlet temperature T_2 [14].

$$COP_{Brayton} = \frac{q_h}{w} = \frac{q_h}{q_h - q_c} = \frac{T_2}{T_2 - T_1} \tag{2}$$

High values of T_1 increase $\mathrm{COP}_{\mathrm{Brayton}}$, but T_1 is limited to the temperature T_0 of the available heat source which can be ambient temperature or an exhaust air stream. It is visible from Eq. (2) that the COP

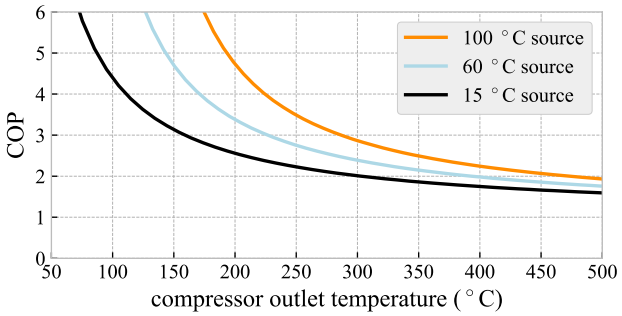

Figure 2: Brayton-cycle COP for high compressor outlet temperatures T_2

decreases with a rising heat sink temperature level and approaches the value of direct electrical heating $COP_{deh} = 1$ for very high T_2.

Figure 2 shows the COP levels of an ideal Brayton cycle heat pump as a function of T_2 for different heat source temperatures $T_0 = T_1$. It shows clearly that the use of exhaust streams is an important aspect when increasing the energy efficiency of industrial processes. The trend of low COP for high sink temperatures also holds for Carnot or Rankine cycle heat pumps [6] and explains why high temperature heat pumps tend to have a lower COP than heat pumps for domestic purpose and low temperatures (see Figure 2 and Table 1).

3. Technical specifications of the DLR-CoBra prototype

With the construction of the prototype 'CoBra' (**Co**ttbus **Bra**yton-cycle heat pump) the German Aerospace Center (DLR) aims at researching the key parameters of a high temperature heat pump with air as working fluid. The high temperature heat pump is designed to provide up to 200 kW of useful heat at temperature levels above 250 °C [15]. Figure 3 shows a model of the heat pump with its most important components. The heat pump has a conditioning unit to control the amount of working fluid in the system consisting of a buffer storage and vacuum pump. Dry air will be used for safety reasons in the research environment. It is non-toxic and has zero global warming potential unlike other common refrigerants [6]. The air in the heat pump must be dried in order to prevent condensation and icing of the turbine at low temperatures.

3.1. Working principle

The compressor increases the pressure and temperature of the working fluid which is the equivalent to state change 1 → 2 of the reverse Brayton cycle (see Figure 1). The high temperature heat exchanger (HTHE) transfers heat to the secondary process which is simulating the industrial process that requires heat. In the turbine, the working fluid is expanded 3 → 4 and power is recovered. The low temperature heat exchanger (LTHE) simulates the heat source which can be ambient air or an exhaust gas stream at higher temperatures. The inlet temperature of the cooling cycle is set to T_0=15 °C for all simulations. The low temperature secondary cycle can also be used for refrigeration at temperatures below 0 °C. The recuperator increases temperature lift at the cost of increased power consumption as shown in Figure 1. It allows to research different operation modes and temperature levels of the heat pump.

Red lines indicate high pressure, blue lines indicate low pressure. Both are fully independent of the ambient air pressure. By filling more working fluid from the buffer storage into the primary circuit the overall pressure level, mass flow and power can be increased. This technique is called fluid inventory control and can be used in closed cycle Brayton engines without combustion [9]. The air buffer also accounts for leakages of the working fluid in the turbomachines and ensures a constant pressure level for repeatable operating conditions.

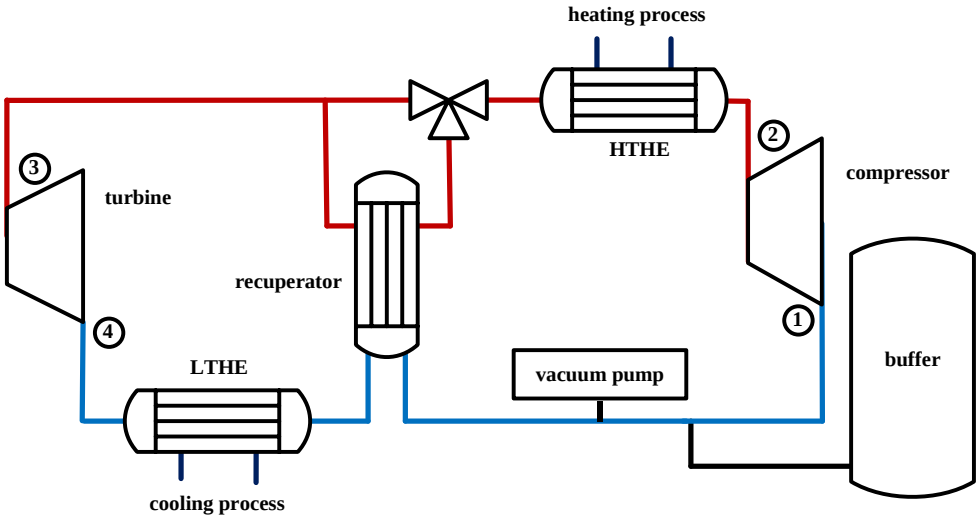

Figure 3: Simplified piping and instrumentation diagram of the Brayton cycle heat pump of the DLR Institute of Low-Carbon Industrial Processes in Cottbus (Germany)

3.2. Part load strategy

In order to meet a reduced heat demand below nominal load, the heat pump can adjust the thermal output with two different control strategies:

- Shaft speed control (SSC)
- Fluid inventory control (FIC)

Reducing the compressor shaft speed yields lower pressure and temperature ratios, lower mass flow and reduces the heat delivery of the heat pump. The compressor outlet temperature T_2 is reduced (see Figure 1). Using fluid inventory control the temperature levels of the thermodynamic process can be kept constant at different load levels. Pradeep Kumar et al. [9] have shown for a closed Brayton cycle gas turbine that fluid inventory control as a part load strategy allows much higher efficiencies than changing temperature levels or bypassing parts of the gas stream.

4. Methodology

In order to simulate the part load performance of the heat pump, a thermodynamic performance model of the system has been developed. The performance model accounts for the effects that occur during part load operation of a closed-cycle heat pump system. The following subsections outline the methods used for the analysis.

Simulations were mainly carried out on a system level. Detailed component simulations are not required to assess the system behavior and were left out of the present work. As the development of the heat pump and simulation tools progresses, higher-fidelity methods will be developed for more in-depth analyses.

4.1. Heat pump cycle simulation

The steady-state heat pump model on which the present analyses are based was created using the DLR in-house performance code GTlab-Performance developed by Becker et at. [16]. In the 0D thermodynamic cycle simulation, the main components of the heat pump are represented as modules, which in turn model the changes of thermodynamic state in the working medium.

For off-design calculations, a performance map of the compressor particularly developed for the CoBra prototype heat pump was used. The map is the result of detailed 3D CFD simulations of the flow in the compressor stages, which used the exact geometry of the blades. The turbine performance map was generated by scaling an existing turbine map of a gas turbine to match the turbine performance of the CoBra prototype based on 3D CFD simulation data computed with the preliminary turbine geometry.

In order to estimate the transferred heat of the shell-and-tube heat exchangers, an approach based on the Number of Transfer Units (NTU) method has been implemented using correlations from VDI Heat Atlas [17].

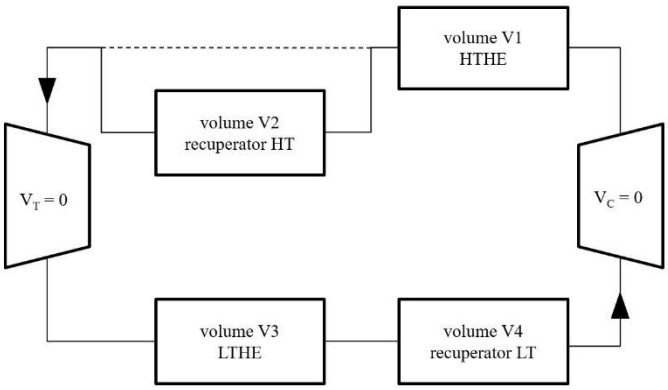

Figure 4: Heat pump component volumes for calculation of pressure levels

The heat transfer is calculated from the two inlet flows and the heat exchanger geometry and accounts for variations in similarity parameters such as Nusselt and Reynolds number. The thermodynamic cycle simulation is coupled with the heat transfer simulation in order to model the system behavior under different operating conditions.

4.2. Pressure level estimation depending on fluid inventory

A simplified heat pump model is used to calculate fluid mass on the high and low pressure side of the heat pump under stationary operating conditions. The volumes are mainly determined by the geometry of the heat exchangers and piping. The pipe volume is lumped to the heat exchangers. According to this, four volumes represent the heat pump components as shown in Figure 4. Due to their small size turbomachine volumes are neglected. Fluid mass is calculated using the semi-ideal gas model of GTlab-Performance, which provides values for density at the inlet and outlet stations of these volumes.

$$M_{Fluid} = \sum_{i=1}^{n=4} V_i \, \bar{\rho}_i \tag{3}$$

M_{Fluid} is approximated with the approach shown in Eq. (3) by using the arithmetic mean value of densities $\bar{\rho}_i$ for each volume V_i. This method is coupled with the GTlab-Performance solver by an iterative correction of lower pressure level for a user-defined fluid inventory. At nominal load the total pressure at compressor inlet is set to the design value of $p_{1,nominal} = 101325\ Pa$.
Part load operating conditions lead to a variation of compressor inlet flow conditions. Reducing compressor shaft speed shifts the operating point to lower pressure ratios, which in most cases induces rising lower pressure levels in hermetic systems. For system level simulations of Brayton cycle heat pumps, it can be important to consider this effect to correctly predict power input and operating limits.

4.3. Pressure drop approximation at partial load

In addition to the isentropic efficiency of turbomachines, pressure drop is a significant factor for the overall heat pump performance. In Brayton cycle heat pumps, the energy recovery of the turbine strongly depends on the pressure losses in the system. This effect is taken into consideration by a pressure loss coefficient ζ_i for each component:

$$\Delta p_i = \zeta_i \frac{\rho_i}{2} c_i^2 \tag{4}$$

Pressure drop is mainly driven by friction losses in heat exchangers, valves and piping. As the heat pump is still under development, not all component geometries and no experimental data are available. Therefore, a simplified approach is used to approximate part load pressure drop in this work. A reference pressure drop for the high and low pressure side of the heat pump is calculated for design operating conditions based on data from the component manufacturers. Pressure drop coefficient ζ is considered to be constant because relevant Reynolds numbers are sufficiently high in all operating conditions (see Moody chart e.g. [17]).

$$\frac{\zeta}{2\,A^2} = \Delta p_{ref}\,\frac{\rho_{ref}}{\dot{m}_{ref}^2} = const. = C_\zeta \tag{5}$$

Off-design pressure drop is estimated by deriving the part load value from the reference state depending on actual mass flow and fluid density. This approach allows a calculation with the parameter set of the GTlab-Performance model:

$$\Delta p = C_\zeta\,\frac{\dot{m}^2}{\rho} = \Delta p_{ref}\,\frac{\dot{m}^2}{\dot{m}_{ref}^2}\,\frac{\rho_{ref}}{\rho} \tag{6}$$

According to the method introduced, pressure losses are approximated for each stationary operating point. On the high pressure side the resulting pressure drop is applied upstream of the turbine inlet and on low pressure side upstream of compressor inlet.

4.4. Reynolds number effect on efficiency of turbomachinery

In compressor and turbine maps, the effect of Reynolds number on the performance of turbomachinery is usually neglected. However, the increased kinematic viscosity at low Reynolds numbers results in additional losses or lower efficiencies. Multiple efficiency scaling correlations have been proposed to account for the Reynolds number effect. The general form of the efficiency correction follows [18]:

$$\frac{1-\eta}{1-\eta_{ref}} = a + (1-a)\left(\frac{Re}{Re_{ref}}\right)^n \tag{7}$$

In Eq. (7), the coefficient a denotes the fraction of the losses that are independent of the Reynolds number. The exponent n is a measure for the Reynolds number dependence of the losses. The effect of Reynolds number on turbomachine efficiency is shown in Figure 5 for three commonly used correlations taken from Wiesner [18] .

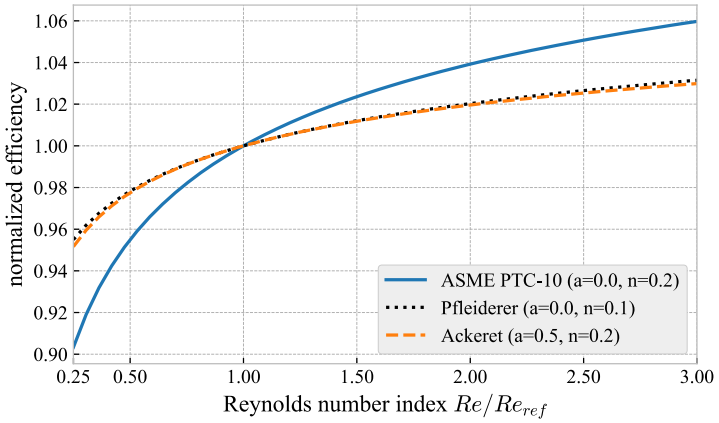

Figure 5: Effect of Reynolds number on turbomachine efficiency based on selected correlations [18]

The ASME Performance Test Code 10 [19] provides Reynolds number correction correlations for axial and centrifugal compressors. Axial compressor efficiencies are assumed to scale only with the Reynolds number ratio, resulting in values of $a = 0$ and $n = 0.2$. Since experimental data of the turbomachines were not available at the time of this study, the coefficients proposed in ASME PTC-10 were applied for the present analyses.

5. Results and discussion

To investigate the part-load capability of closed-cycle high temperature heat pumps two strategies are evaluated (see section 3.2):

- Shaft speed control (SSC): Operating areas of HTHP for non-recuperated and recuperated cycle
- Fluid inventory control (FIC): Comparison with SSC for a scenario with constant temperature requirement and load reduction by 75%

5.1. Operating limits of Brayton cycle heat pumps controlled by shaft speed

The permissible operating range of the CoBra prototype heat pump is bounded by several operating limits:

- Compressor surge: The surge line marks the operating limit beyond which no stable flow can be sustained in the compressor due to flow separation at the blades. A certain safety margin must be kept during operation.
- Maximum shaft speed: The absolute shaft speed is typically limited by the mechanical strength of the rotor blades.
- Secondary mass flow: The secondary mass flow rate at the heat exchanger's secondary side is bounded by the minimum and maximum delivery rate of the fan.
- Maximum compressor inlet temperature: Due to the used instrumentation, the compressor inlet temperature must not exceed a maximum value.
- Compressor choke: At high corrected mass flow rates, the flow reaches sonic velocities, preventing further increase of mass flow rate.

Using the methods presented in section 4, the operating envelopes have been calculated for the CoBra prototype heat pump in non-recuperated and recuperated operating mode. The results are shown in Figure 6 (a) and (b), respectively.

The COP used for the following analysis is defined in Eq. (8) and computed with consideration of pressure drop and component efficiencies as described in section 4:

$$COP = \frac{\dot{Q}_{HTHE}}{P_C - P_T} \tag{8}$$

A comparison of the operating modes shows that the recuperated cycle allows for operation at higher process temperatures and thermal output. In accordance with the assessments in section 2.2, both envelopes show a decrease of COP when higher temperatures are demanded. It should be noted that the non-recuperated cycle shows an operating area where the COP drops below 1: At these operating points, the turbine outlet temperature exceeds the temperature of the heat source level $T_0 = 15\,°C$. Therefore, heat is rejected at both heat exchangers and the system is not working as a heat pump. When comparing the operating envelopes, the recuperated cycle shows higher COPs at the same delivered heat flows and temperatures.

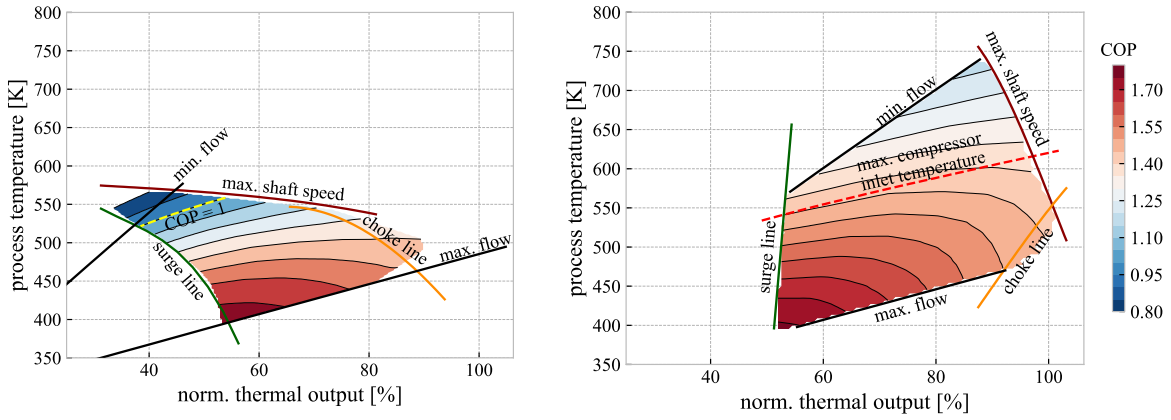

(a) Non-recuperated (b) Recuperated

Figure 6: Operating envelopes with COP

Figure 7 illustrates the heat pump's permissible operating range with the current instrumentation for a given fluid inventory in a single diagram. The achievable temperatures are currently limited by the instrumentation at the compressor inlet. Higher delivery temperatures may be achieved by modifying the installed sensors. It is noticeable that the delivered heat flow cannot be reduced below a minimum value by shaft speed control.

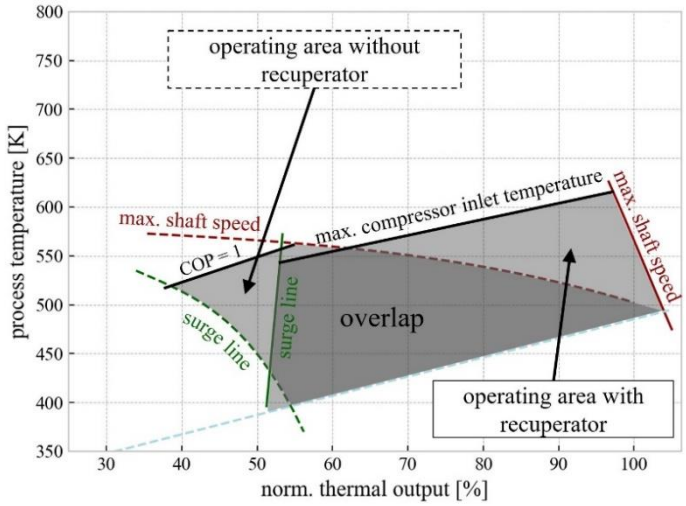

Figure 7: Comparison of operating areas depending on process architecture

Consequently, if a process requires a wider operating range, additional control options are necessary. This is shown in the following section, where the limitations of the recuperated process with fixed amount of working fluid are compared to a system with fluid inventory control.

5.2. Fluid inventory control

As discussed in section 5.1 load reduction of shaft-speed-controlled high temperature heat pumps is limited e.g. due to instability of the compressor. Fluid inventory control has the potential to significantly expand the operating range with little variation in engine efficiency (see section 3.2).

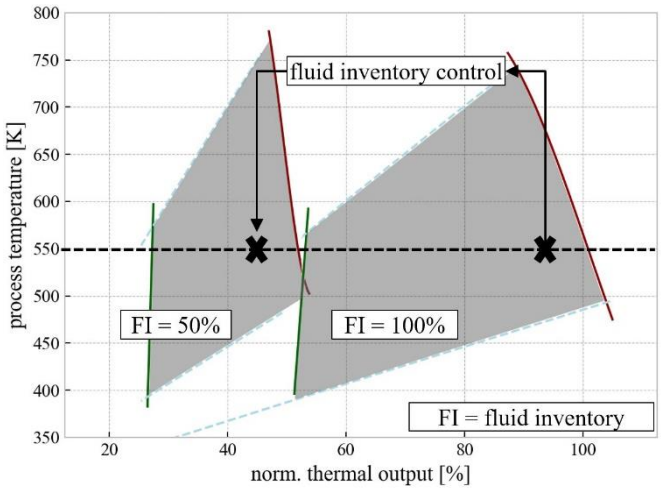

Figure 8: Effect of fluid inventory variation on operating limits of recuperated cycle

Figure 8 shows the effect of a variable fluid inventory on the operating envelope of a HTHP. Altering fluid mass shifts the resulting operating area to corresponding power outputs. When reducing the fluid inventory from a reference state to 50% as shown in the example, the thermal output scales almost linearly with the fluid mass while the temperature range remains almost identical.
For the investigations presented in this paper, a required process temperature of 550 K is assumed. The thermal output range extends from the nominal load to a reduction of 75%. However, the recuperated process architecture only allows a reduction to approx. 55% of nominal load via control of compressor rotational speed.

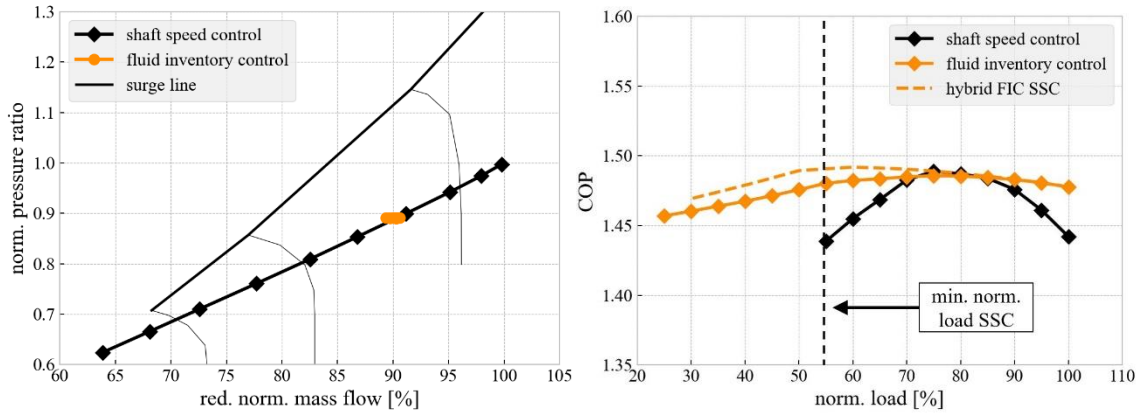

(a) Compressor map (b) COP

Figure 9: Fluid inventory control vs. shaft speed control for load reduction

If the process requires greater flexibility, the fluid inventory must be adjusted accordingly. This is demonstrated in this figure by shifting an operating point through FIC to low thermal output, which could not be reached by reduction of shaft speed.

Figure 9 demonstrates the advantages of part load operation with fluid inventory control. Figure 9 (a) shows a section of the compressor map. The black working line connects the operating points in the case where part load operation is controlled by varying the compressor rotational speed. For each operating point, the required process temperature is set to 550 K. The inlet temperature of the secondary side of both heat exchangers (HTHE and LTHE, see Figure 3) is 15 °C. The amount of working fluid is optimized for best COP in this range.

When thermal output is controlled by adjusting the fluid inventory, the operating conditions in the turbomachines remain almost identical for the requested performance range. The resulting operating point has been determined by optimization of COP near nominal load conditions and is highlighted in orange in Figure 9 (a).

Figure 9 (b) compares the COP for the entire operating range of shaft speed control and FIC. It becomes clear, that an adjustment of fluid inventory is not only able to extend the operating range but also leads to only minor deviation of heat pump performance even for very low thermal output. The decreasing COP is mainly evoked by Reynolds corrections (see section 4.4) which lead to lower efficiencies of the turbomachines for low-power operating conditions. This trend coincides well with the results by Pradeep Kumar et al. [9], who investigated fluid inventory control for closed cycle gas turbines. There is also some optimization potential by introducing a hybrid method where fluid inventory is controlled as well as compressor shaft speed. This is shown by the dotted orange line. Therefore, fluid inventory control should be considered to increase flexibility of future high temperature heat pumps and extend the scope of their potential applications.

6. Conclusion and outlook

High temperature heat pumps can cover a wide range of industrial process heat requirements. They highlight a very efficient decarbonization strategy for process heat temperatures up to at least 500 °C. Closed cycle Brayton heat pumps capable of thermal output regulation by fluid inventory control provide high flexibility while operating with almost constant efficiency. It is shown that heat pumps are limited to a certain operating range depending on the available methods to control part load operation. Maximum output is mainly determined by thermal and mechanical load capacity of the components.

Two strategies for load reduction have been investigated in the scope of this work. If the heat pump is solely controlled by variation of shaft speed, the permissible minimum load is limited e.g. by compressor stability. The overall operating range for non-recuperated and recuperated process architecture is demonstrated by the introduction of HTHP envelopes. For the CoBra prototype heat pump the recuperator invokes higher output temperatures and better COP.

In order to demonstrate the field of application for fluid inventory control, a scenario with constant output temperature and a load reduction down to 25% has been investigated. The simulation results indicate that fluid inventory control incurs only minor reduction of heat pump performance over the entire operating range. On the other hand, the shaft speed controlled heat pump with fixed amount of working fluid can only operate down to 55% load with varying operating conditions and efficiency.

Fluid inventory control is a promising method to control thermal output of highly flexible future heat pumps. It offers an effective mechanism to react to heat demand changes and address grid fluctuations. Its effect on the transient stability of the compressor will be researched during the operation of the CoBra. In order to investigate fluid inventory control in more detail, studies based on this work with a higher-fidelity model base and experimental examinations are planned.

Acknowledgements

The authors thank Enrico Jende, Leander Schleuss, Panagiotis Stathopoulos and all members of the department of high temperature heat pumps for their support.

References

[1] R. de Boer, A. Marina, B. Zühlsdorf, C. Arpagaus, M. Bantle, V. Wilk, B. Elmegaard, J. Corberán and J. Benson, "Industrial Heat Pump Whitepaper," SINTEF, 2020.

[2] Fraunhofer Institute for Systems and Innovation Research, Fraunhofer Institute for Solar Energy Systems, "Mapping and analyses of the current and future (2020-2030) heating/cooling fuel deployment (fossil/renewables)," report prepared for the European Commission, 2016.

[3] M. Rehfeldt, T. Fleiter and F. Toro, "A bottom-up estimation of the heating and cooling demand in European industry," *Energy Efficiency*, pp. 11:1057-1082, 2018.

[4] European Union, "Long-term low greenhouse gas emission development strategy of the EU and its Member States," 06 03 2020. [Online]. Available: https://unfccc.int/documents/210328.

[5] Prognos, Öko-Institut, Wuppertal-Institut, "Towards a Climate-Neutral Germany," Executive Summary conducted for Agora Energiewende, Agora Verkehrswende and Stiftung Klimaneutralität, [Full study in German language only], 2020.

[6] C. Arpagaus, F. Bless, M. Uhlmann and J. Schiffmann, "High temperature heat pumps: Market overview, state of the art, research status, refrigerants, and application potentials," *Energy*, pp. 985-1010, June 2018.

[7] V. Aga, E. Conte, R. Carroni, B. Burcker and M. Ramond, "Supercritical CO2-Based Heat Pump Cycle for Electrical Energy Storage for Utility Scale Dispatchable Renewable Energy Power Plants," in *5th Int. Supercrit. CO2 Power Cycles Symp*, San Antonio Texas, 2016.

[8] R. B. Laughlin, "Pumped thermal grid storage with heat exchange," *Journal of Renewable and Sustainable Energy*, 02 August 2017.

[9] K. Pradeep Kumar, A. Tourlidakis and P. Pilidis, "Performance review: PBMR closed cycle gas turbine power plant," International Atomic Energy Agency, Vienna (Austria), 2001.

[10] E. Agelidou, M. Henke, T. Monz and M. Aigner, "Numerical Investigation of an Inverted Brayton Cycle Micro Gas Turbine based on Experimental Data," in *Proceedings of ASME Turbo Expo 2018 - Turbomachinery Technical Conference and Exposition*, Oslo, Norway, 2018.

[11] M. Götz, J. Lefebvre, F. Mörs, A. McDaniel Koch, F. Graf, S. Bajohr, R. Reimert and T. Kolb, "Renewable Power-to-Gas: A technological and economic review," *Renewable Energy*, pp. 1371-1390, 2016.

[12] B. Zühlsdorf, F. Bühler, B. M. and B. Elmegaard, "Analysis of technologies and potentials for heat pump-based preocess heat supply above 150 °C," *Energy Conversion and Management: X*, 2019.

[13] BASF, "BASF Carbon Management," 07 2020. [Online]. Available: https://www.basf.com/global/en/who-we-are/sustainability/we-produce-safely-and-efficiently/energy-and-climate-protection/carbon-management.html. [Accessed 12 11 2020].

[14] B. Weigand, J. Köhler and J. von Wolfersdorf, Thermodynamik kompakt, Heidelberg Dordrecht London New York: Springer, 2010.

[15] L. Schleuss, T. Lorenz, D. Wenzke, C. Hensel, S. Panagiotis, E. Nicke and U. Riedel, "Decarbonisation of industrial processes - New DLR institute in Cottbus and Zittau," in *4th International Conferene on Energy Supply and Energy Efficiency*, Baku (Azerbaijan), 2020.

[16] R.-G. Becker, F. Wolters, M. Nauroz and T. Otten, "Development of a Gas Turbine Performance Code

and Its Application to Preliminary Engine Design," *DLRK,* 27-29 09 2011.

[17] VDI e. V., VDI Heat Atlas, Berlin: Springer, 2010.

[18] F. Wiesner, "A New Appraisal of Reynolds Number Effects on Centrifugal Compressor Performance," *Journal of Engineering for Power,* pp. 384-392, 07 1979.

[19] The American Society of Mechanical Engineers, Performance Test Code on Compressors and Exhausters (ASME PTC-10), New York: ASME, 1997.